3.2.5 The phylogeny of *Sericania*

To investigate evolution of Himalayan faunas as a whole, subordinate patterns may provide important information, such as found in many xerophilous forms, invading the Himalaya from the west (Mani 1968) to the east and becoming a dominant element of the alpine fauna and flora. This alpine element is as far as known (Ahrens 2004b) lacking in the Sericini, but this general pattern (Martens 1993) is supposed to be modified in case of the genus *Sericania*, being with one species group (*S. kashmirensis*-group) restricted to the steppe forest of the North-West Himalaya and extending their ranges only little easterly into Central Himalaya.

Sericania is with its 65 known species a comparatively diverse sericine taxon. The taxonomy and distribution of the Himalayan species has been revised recently (Ahrens 2004b), while the taxa of the Asian mainland were reviewed by Nomura (1976). The here presented cladistic analysis was conducted to shed some light on the relationships among *Sericania* and Sericini, but in particular to investigate evolutionary processes of Himalayan organisms.

Material and methods

Taxon sampling and characters

Thirty-three species belonging to six genera were included in the cladistic analysis, with *Pleophylla* sp. chosen as the outgroup taxon due to their rather close relationship to the ingroup taxa, but with a high probability of not being part of the ingroup (chapter 3.1).

Description, coding and illustration of characters was based on 36 species belonging to six genera (see appendix A 3.2.5). The choice of taxa to be included into ingroup was mainly based on present classification of the *Sericania* species (Nomura 1976) and preliminarily hypothesized relatives, with species included additionally into *Sericania* (Ahrens 2004b). Fifty-six adult characters were scored. The character states are illustrated in Figs 73 and 74.

Phylogenetic analysis

The 66 characters (50 binary and 16 multistate) were all unordered and equally weighted. Inapplicable characters were coded as „-", while unknown character states were coded as „?" (Strong and Lipscomb 1999). The parsimony analysis was performed in NONA 2.0 (Goloboff 1999) using the parsimony ratchet (Nixon 1999) implemented in NONA, run with WINCLADA vs. 1.00.08 (Nixon 2002) as a shell program. Two hundred iterations were performed (one tree hold per iteration) repeating the search ten times. The number of characters to be sampled for reweighting during the parsimony ratchet was determined to be five. All searches were done under the collapsing option "ambiguous" which collapses every node with a minimum length of 0. State transformations were considered to be apomorphies of a given node only if they were unambiguous (i.e., without arbitrary selection of accelerated or delayed optimization) and if they were shared by all dichotomised most parsimonious trees.

Bremer support (Bremer 1988, 1994) and bootstrap values (Felsenstein 1985) were evaluated using NONA. Bootstrap analyses of data were performed with 200 replicates using TBR branch swapping. The search was set to a Bremer support level of 12, with seven runs (each holding a number of trees from 100 to 500 times multiple of suboptimal tree length augmentation) and a total hold of 8000 trees. Character changes were mapped on the consensus tree using WINCLADA.

Successive weighting (Farris 1969) was used to further evaluate phylogenetic relationships. This method uses *post hoc* character weighting based on the fit of each character as applied to the trees currently in memory. Thus, the 'quality' of the character data

is used rather than intuitive feeling regarding weighting of characters. Although this method increases the assumptions in the analysis (Siebert 1992), it is useful for analysing phylogenetic pattern when characters exhibit a high level of homoplasy. Characters were reweighted based on the consistency index. The base weight was set at 100. Weights were inserted into NONA parsimony ratchet search via the WINCLADA surface manually. Tree searches continued until the character weights no longer changed (Farris 1988) or until identical trees were found in consecutive searches (indicating stability in the trees).

Characters and character states

In describing character states, I refrain from formulating any hypothesis about their transformation. In particular, coding does not implying whether a state is derived or ancestral. The data matrix is presented in the appendix B 3.2.5.

Head
1. *Surface of the body*: (0) with dull cover of microtrichomes (Fig. 73A); (1) shiny, without dull cover of microtrichomes (Figs 73B-D).
2. *Body, colour*: (0) head + pronotum of the same colour as elytra (Figs 73A-C); (1) head + pronotum of different colour to elytra (Fig. 73D).
3. *Body, colour of ventral face*: (0) reddish or dark brown; (1) yellowish; (2) black.
4. *Anterior margin of labroclypeus medially*: (0) distinctly sinuate; (1) very shallowly sinuate.
5. *Labroclypeus, basis*: (0) completely shiny; (1) dull.
6. *Surface of labroclypeus*: (0) flat (Figs 73F,H); (1) convexly elevate medially (Fig. 73G, arrow); (2) transversely elevate medially (Fig. 73E, arrow).
7. *Frons*: (0) dull; (1) completely shiny.
8. *Frons*: (0) with a few single setae behind frontoclypeal suture (Figs 73E,G,H); (1) completely covered by long setae (Fig. 73F).
9. *Eyes in male*: (0) medium sized, ratio of diameter/ interocular width ~ 0.7-0.5 (Figs 73E,G); (1) small, ratio of diameter/ interocular width < 0.5 (Fig. 73F); (2) very large, ratio of diameter/ interocular width ~ 0.8 (Fig. 73H).
10. *Head, postocular furrow*: (0) strong; (1) absent.
11. *Total number of antennomeres*: (0) ten; (1) nine (CI: 0.5, RI: 0.83).
12. *Antenna, number of antennomeres of clavus in male*: (0) three; (1) four; (2) five; (3) six; (4) seven.
13. *Antenna, clavus in male*: (0) shorter than total maximal width of labroclypeus (Figs 73B,D); (1) longer than total maximal width of labroclypeus (Figs 73A,C).
14. *Antenna, number of antennomeres of clavus in female*: (0) three; (1) four; (2) five.
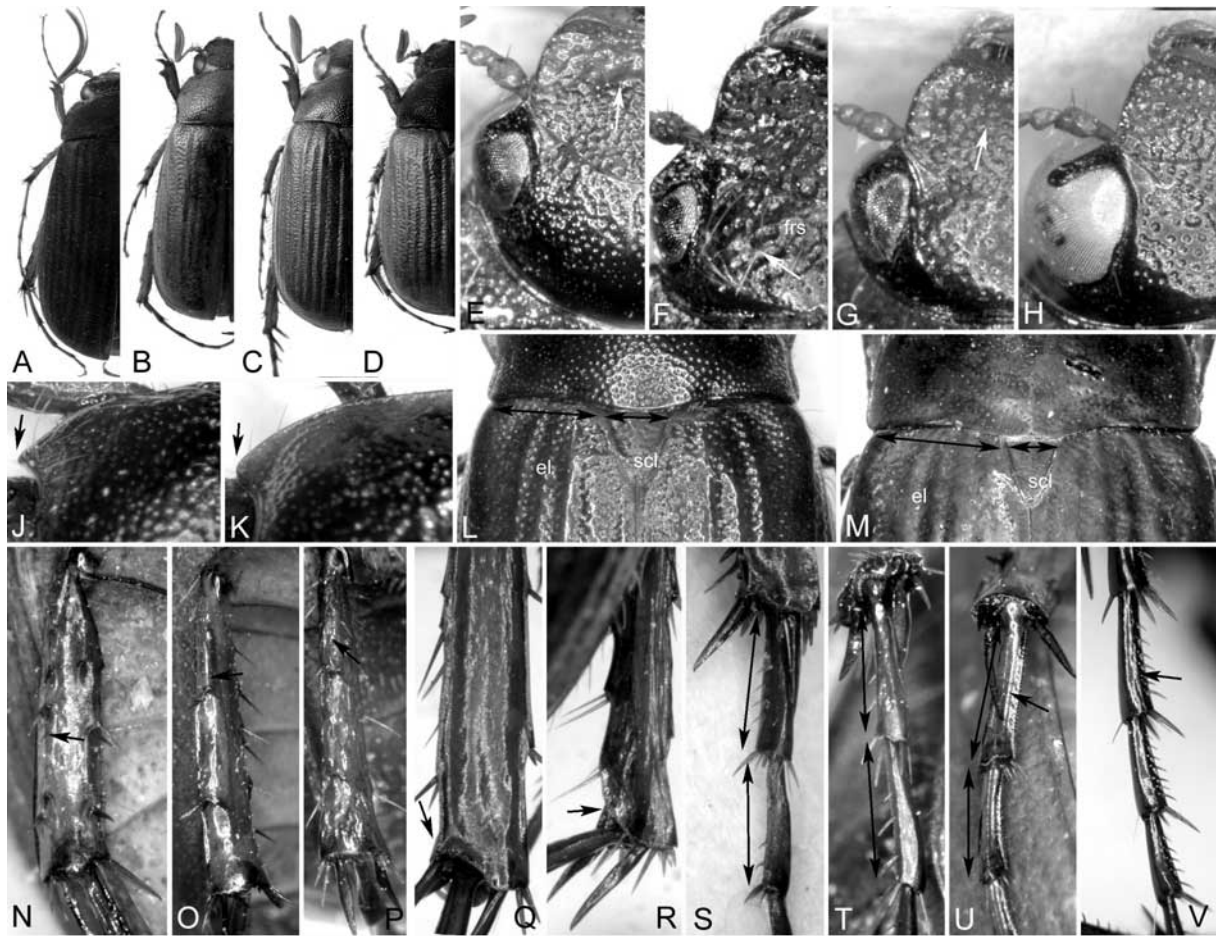
Thorax
15. *Pronotum, anterior marginal line*: (0) present; (1) absent.
16. *Pronotum, anterior angles*: (0) blunt and weakly produced (Fig. 73K); (1) sharp and strong produced (Fig. 73J).
17. *Apical margin of elytra*: (0) without short microtrichomes; (1) with short microtrichomes.
18. *Scutellum in comparison to elytral base*: (0) wide (Fig. 73L); (1) narrow (Fig. 73M).

Legs
19. *Metacoxa*: (0) not transversely impressed; (1) transversely impressed.
20. *Metacoxa, ventral surface*: (0) glabrous, only laterally a few setae; (1) with long and dense setae.

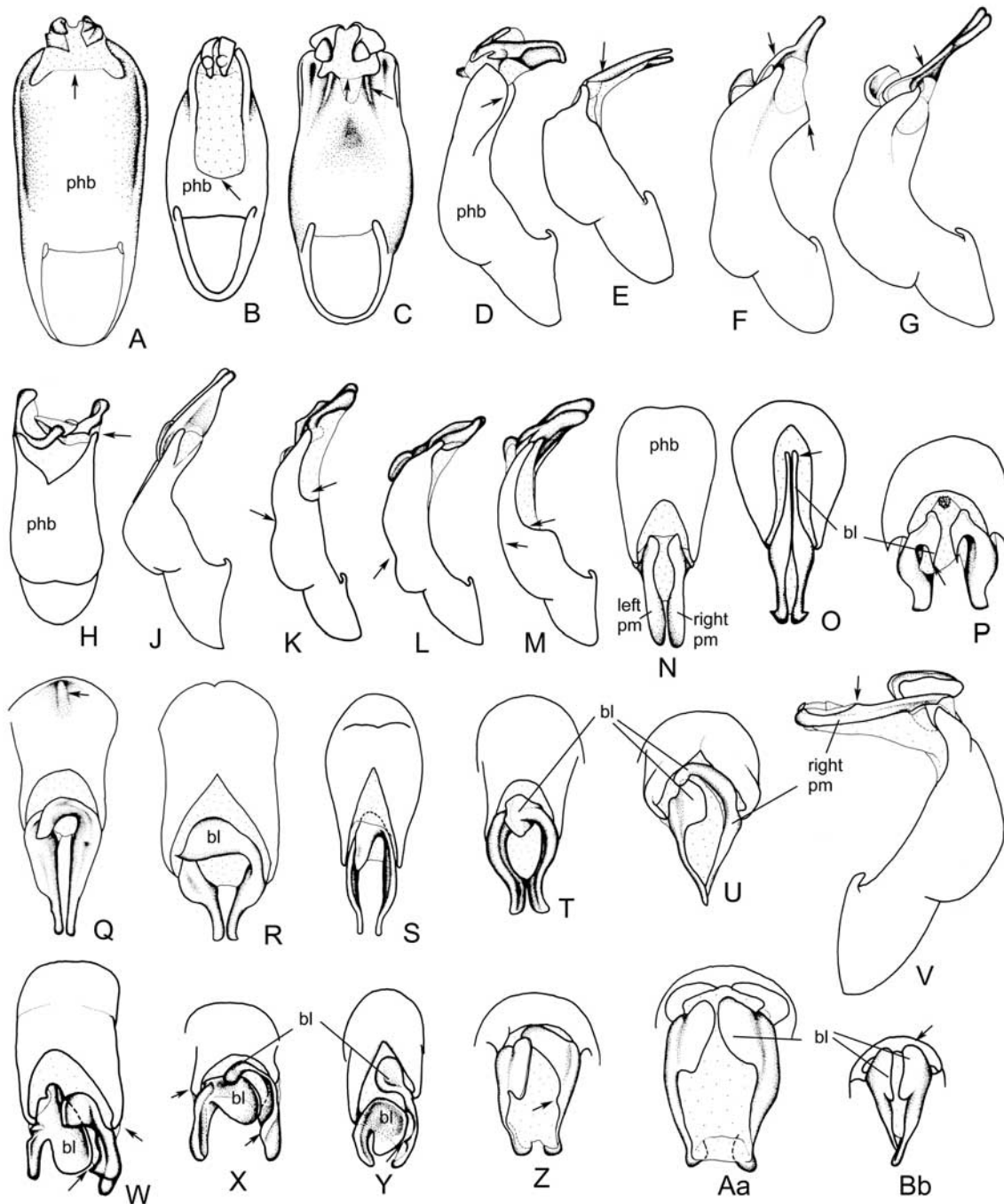21. *Dorsal posterior margin of metafemur*: (0) smooth; (1) serrate.

Fig. 73. A: *Nepaloserica goomensis*; **B:** *Sericania mara*; **C, H, L:** *S. laeticula*; **D, F, J, S:** *S. piattellai*; **E, K, P, R, T:** *S. fuscolineata*; **G:** *S. khagana*; **M:** *S. yamauchii*; **N, U:** *Nipponoserica koltzei*; **O, Q:** *N. procera rufescens*; **V:** *Maladera holosericea*. **A-D:** habitus, dorsal view; **E-H:** head, dorsal view; **J, K:** pronotum, right half, dorsal view; **L, M:** pronotum, scutellum, and elytral base, dorsal view; **N:** metatibia, lateral view; **O, P:** metatibia, dorsolateral view; **Q, R:** metatibia, medial view (detail); **S-V:** basal metatarsomeres, (**S:** medial view, **T-V:** lateral view) (not to scale).

22. *Ventral posterior margin of metafemur in apical half*: (0) smooth (at most in the apical quarter minutely serrate); (1) serrate.
23. *Metatibia dorsally*: (0) not carinate; (1) sharply carinate over all of its length; (2) carinate just in apical portion.
24. *Metatibia, longitudinal carina on lateral face*: (0) absent (Fig. 73P); (1) present in about two third of metatibial length (Fig. 73N); (2) present in basal third of metatibial length (Fig. 73O).
25. *Metatibia, apex interiorly close to tarsal articulation*: (0) bluntly angled, weakly concavely sinuate (Fig. 73S); (1) moderately truncate (Fig. 73Q); (2) sharply incised and strongly truncate (Fig. 73R).
26. *Interior spines on apical face of metatibia*: (0) present; (1) absent.
27. *Tarsi dorsally*: (0) smooth (Figs 73S-U); (1) punctate.
28. *Basal metatarsomere*: (0) longer than the subsequent tarsomere (Figs 73S,U); (1) as long as the subsequent tarsomere (Fig. 73T).
29. *Metatarsomeres, subventral longitudinal carina beside serrate ventral ridge*: (0) present (Fig. 73V); (1) absent (Fig. 73U).
30. *Basal tooth of tarsal claws apically*: (0) all sharply pointed; (1) all bluntly truncate; (2) claws of anterior tarsomeres bluntly truncate.

Male genitalia

31. *Aedeagus, phallobase*: (0) symmetrical (Figs 74A-C,N-P); (1) asymmetrical (Figs 74Q-Bb).
32. *Aedeagus, apex of phallobase ventrally*: (0) not produced into a ventrolateral lobe (Figs 74E-G); (1) produced into a ventrolateral lobe (Fig. 74D, arrow).
33. *Aedeagus, lateral sinuation before insertion of parameres ventrally*: (0) moderately deep (Figs 74A,C,F,G); (1) very deep, almost half of length of phallobase (Figs 74K,M).
34. *Aedeagus, phallobase ventroapically*: (0) not produced into two ventromedian carinae (Figs 74A,B,E); (1) produced into two ventromedian carinae (Fig. 74C, right arrow).
35. *Ventral carina of phallobase*: (0) weakly elevate (Figs 74D,G,J); (1) strongly elevate (more than half as high as dorsoventral extension of phallobase at this position) (Fig. 74F, lower arrow).
36. *Aedeagus, apex of phallobase (lateral view)*: (0) straight to weakly curved ventrally (Figs 74D-G,J,K); (1) strongly curved ventrally in apical third (Figs 74L,M).
37. *Sclerotized portion of ventral phallobase apically*: (0) deeply and narrowly sinuate (Fig. 74B); (1) convexly produced medially (Figs 74A,C).
38. *Aedeagus, phallobase dorsally*: (0) longitudinally convex (Figs 74N-P,R-Bb); (1) with a median longitudinal keel (Fig. 74Q).
39. *Aedeagus, phallobase dorsally (lateral view)*: (0) evenly curved or plain (Figs 74D-G,J,M); (1) distinctly impressed (Figs 74K,L, left arrow).
40. *Aedeagus, dorsal impression of phallobase (lateral view)*: (0) at middle (Fig. 74K); (1) at basal third (Fig. 74L).
41. *Insertion of right paramere*: (0) at the same level as the left (Figs 74A-C); (1) more distal than the left paramere (Figs 74X,Y); (2) more basal than the left paramere (Fig. 74W).
42. *Parameres*: (0) symmetrical (Figs 74B,O,P); (1) asymmetrical (Figs 74Q-Bb).
43. *Parameres laterally*: (0) longitudinally convex (Figs 74D,E,K-M); (1) with a lateral keel, which is strongly produced and dorsoventrally flattened (Figs 74F,G, arrow).
44. *Parameres along all of its length*: (0) straight (Figs 74N,O,Q); (1) weakly curved inward (Figs 74R,S); (2) strongly curved inward (Figs 74P,T); (3) left paramere bent inward (Figs 74W,Y).
45. *Left paramere, basal lobe*: (0) absent (Fig. 74N); (1) present (Figs 74O-Bb).
46. *Left paramere, basal lobe*: (0) slender and long (longer than wide) (Fig. 74O); (1) large, circular; (2) very short (mostly covered behind basal lobe of right paramere) (Figs 74Q-T).
47. *Left paramere, basal lobe*: (0) produced basally and hooked at apex (Figs 74U,Aa,Bb); (1) immediately produced basally, not hooked; (2) produced basomedially (Figs 74W-Y); (3) produced basally and distally (Fig. 74P).
48. *Left paramere, basal lobe*: (0) comprising basal quarter of paramere (Figs 74P,X); (1) comprising about basal third or more of paramere (Figs 74W-Bb).
49. *Right paramere, basal lobe*: (0) absent (Fig. 74N); (1) present (Figs 74O-Bb).
50. *Right paramere, basal lobe*: (0) short, at maximum half as long as distal portion of paramere (Figs 74P,Q,S,T,W-Bb); (1) long, almost as long as distal portion of paramere (Figs 74O,R,U).
51. *Right paramere, basal lobe*: (0) convexly rounded at apex (Figs 74Q,T-Bb); (1) sharply pointed at apex (Figs 74O,P,R,S).
52. *Right paramere, basal lobe*: (0) elongate (distinctly longer than wide) (Figs 74O,R,S,U,X); (1) circular (almost as wide as long) (Figs 74W,Y).
53. *Right paramere, small lobe on medial margin*: (0) absent (Figs 74N-U); (1) present (Figs 74V, arrow, W-Z, lower arrow).

Fig. 74. A: *Nepaloserica goomensis*; **B, O:** *Nipponoserica koltzei*; **C:** *S. piattellai*; **D, P:** *S. gilgitensis*; **E, U:** *S. yamauchi*; **F, R:** *S. poonchensis*; **G, Q:** *S. besucheti*; **H, M, X:** *S. kleebergi*; **J, S:** *S. costulata*; **K:** *S. mela*; **L, Y:** *S. nepalensis*; **N:** *Stilbolemma sericea*; **T:** *S. dubiosa*; **V, Aa:** *Sericania* sp. 1; **W:** *S. mara*; **Z:** *S. lewisi*; **Bb:** *Sericania* sp. 2. **A-C:** aedeagus, ventral view; **D-G, J-M:** aedeagus, left side lateral view; **H:** aedeagus, dorsal view; **N-U, W-Bb:** parameres, dorsal view; **V:** aedeagus, right side lateral view (not to scale).

54. *Right paramere, basal lobe*: (0) produced basally (Figs 74Aa,Bb); (1) not produced basally (Figs 74Q-U,Z).
55. *Right paramere, basal lobe directed*: (0) medially (Figs 74Q,R,T,U); (1) distally (Figs 74P,S); (2) basally (Figs 74O,Aa).
56. *Apex of basal lobe of right paramere*: (0) strongly produced distally; (1) not produced at all; (2) strongly produced medially.

Results

The analysis of 56 adult characters with the parsimony ratchet and the above mentioned settings repeating the search ten times yielded 123 equally parsimonious trees of 171 steps (ensemble consistency index (CI): 0.43, ensemble retention index (RI): 0.72). Characters 22, 45, and 49 proved uninformative in the present data set. For each character, the consistency index (ci) and the retention index (ri) calculated by WINCLADA analysis are given in appendix C 3.2.5. The strict consensus of these trees is presented in Fig. 75 with areas of conflict in topology shown as polytomies. The strict consensus tree (Fig. 75) of equally weighted characters exhibits a high level of polytomy most nodes of the *Sericania kashmirensis*- group.

Three major lineages may be recognized from the strict consensus tree (Fig. 75) within the monophyletic clade (node A) of *Sericania*: (1) the *Sericania fuscolineata*-group; (2) the *Sericania nepalensis*-group + *Sericania* sp. 2; and (3) the *Sericania kashmirensis*-group. A sister taxon of *Sericania* was not apparent according to the tree topology of the strict consensus tree. In comparison to the apical nodes of the genus, the support of the node of *Sericania* is relatively low (node A, Bremer support: 1, bootstrap value: 46 %). To assume in some manner information of the high number of equally parsimonious trees resulted from the parsimony ratchet with equally weighted characters, a majority rule consensus tree was generated (Fig. 76).
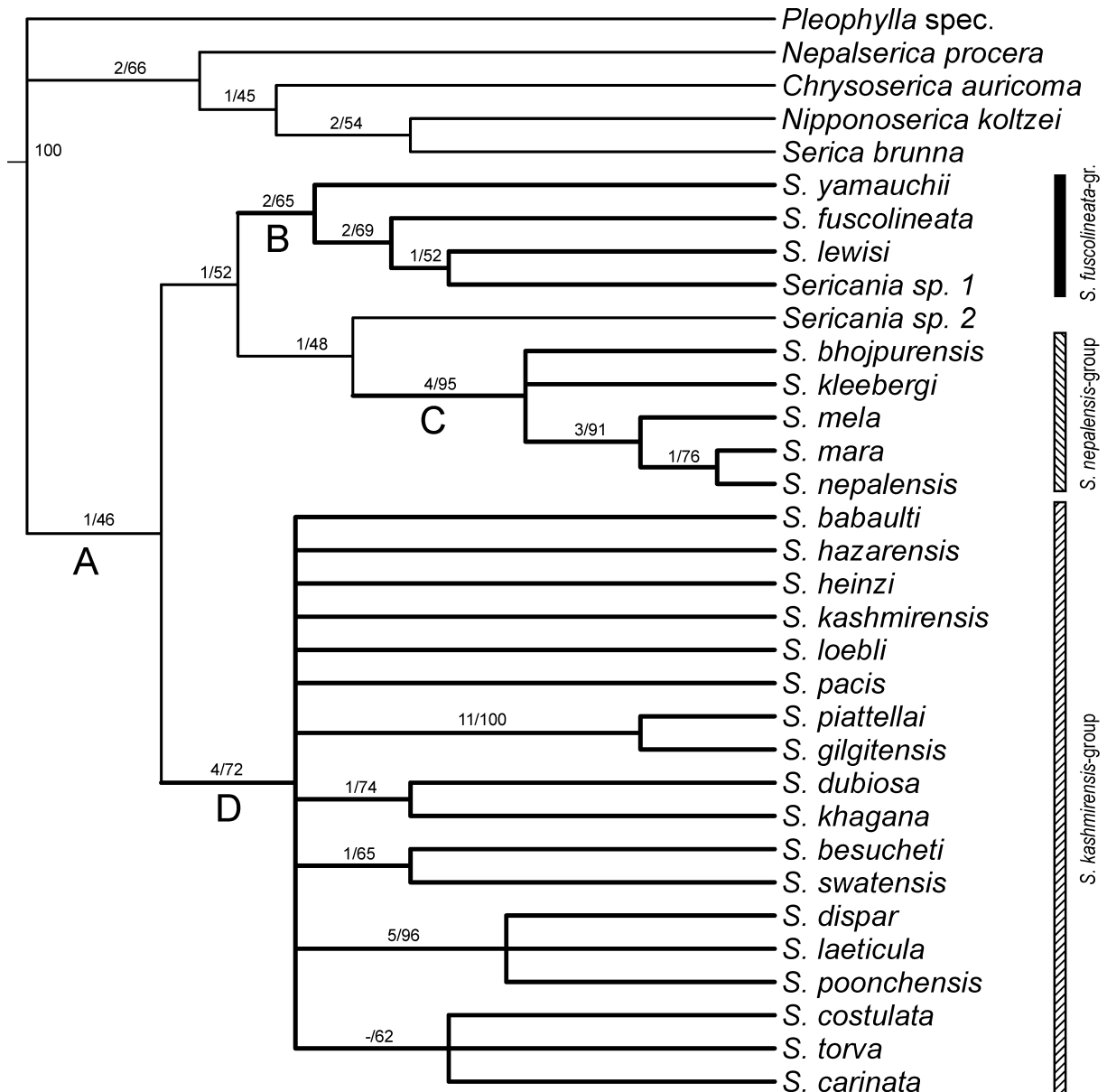
The use of successive approximations character weighting (SACW, Farris 1969) based on consistency index greatly reduced the number of most parsimonious trees (MPTs), producing a significantly more resolved strict consensus tree, especially among the representatives of the *Sericania kashmirensis*-group. In this approach weights no longer changed after two iterations (for weights each iteration see appendix C 3.2.5). From the analysis result six MPTs of 172 steps (CI: 0.55, RI: 0.78), whose strict consensus tree was one step longer (Fig. 77). Although numerous nodes are well supported, especially those of the species groups apparent also from analysis with unweighted characters (Fig. 75, nodes B,C,D), the bootstrap values for the several basal and apical nodes are low also after SACW.

Discussion

Characters and computer analysis

The overall structure of the equally weighted majority rule consensus tree (Fig. 76) is the same as in SACW analyses (Fig. 77), with one separate clade including *Nepaloserica*, *Chrysoserica*, *Nipponoserica* and *Serica*, and a second comprising all species of *Sericania*. Only in the latter clade the topology is altered slightly. Founded on the consistency index based SACW strict consensus tree character evolution and evolutionary diversification of *Sericania* are discussed. Figure 78 illustrates the character changes along each branch under DELTRAN optimization.

Characters of external morphology are in the same manner as male genital characters consistent with the tree topology of the analyses, showing both equilibrated means of consistency index (ci) and retention index (ri) (see appendix C 3.2.5).

Fig. 75. Strict consensus (188 steps, CI: 0.39, RI: 0.67) of the 123 most parsimonious trees with a length of 171 steps (CI: 0.43, RI: 0.72); above each branch support indices (Bremer support/ bootstrap values). *S.* = *Sericania.*
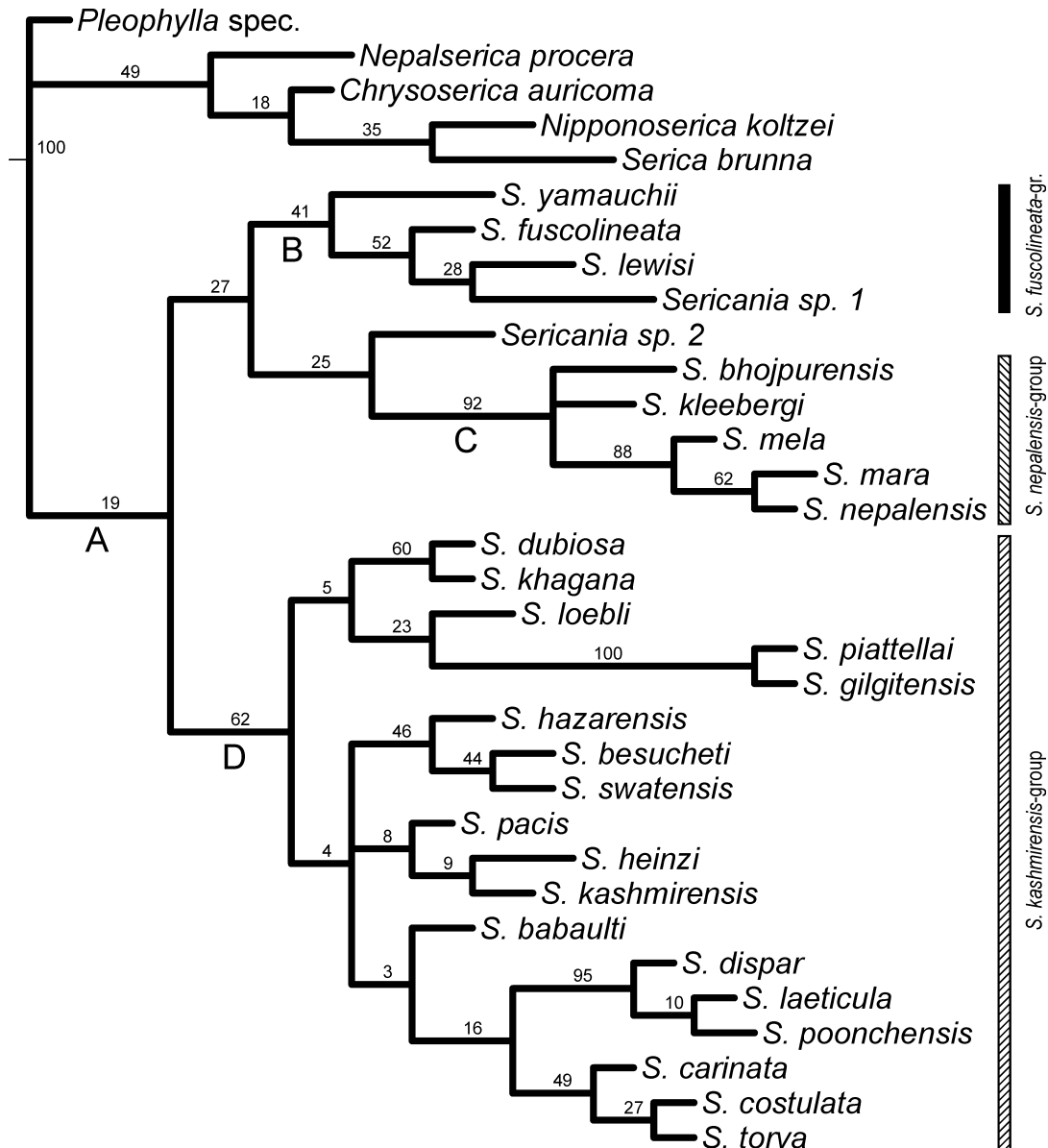
Monophyly of Sericania

Although not exhaustive, this study is the most comprehensive phylogenetic analysis of *Sericania* ever conducted. Due to the high homogeneity in their genital features (Nomura 1976), a large part of the Far East species of *Sericania* has not been considered for the cladistic analyses. All of them, however, share the same apomorphic states as the taxa exemplarily included here at node B. The results improve the current understanding of relationships among the Asian Sericini.

The genus *Sericania* once established by Motschulsky (1860) for a single species, *S. fuscolineata*, comprised little time ago only East Asian species, mainly from the Japanese Archipelago (Medvedev 1952b; Nomura 1976). However, some of these species have been reported recently from northern China, too, and moreover, taxa from Himalaya have been assigned to the genus (Ahrens 2004b).

Monophyly of *Sericania* (node A) including the recently included new taxa from the Himalaya, was evident from both analyses with unweighted and weighted characters (Fig. 75,

77, node A). It is supported by a number of unambiguous apomorphies: (1) surface of labroclypeus convexly elevate medially (6:1); (2) subventral longitudinal carina beside serrate ventral ridge of metatarsomeres absent (29:1); and (3) right paramere with a basal lobe directed medially (55:0).

Fig. 76. Majority rule consensus (172 steps, CI: 0.43, RI: 0.71) of the 123 equally parsimonious trees (171 steps) resulting from parsimony ratchet based on equally weighted characters; above each branch is given the frequency (%) of a node among all MPTs. *S. = Sericania*.

The search for the sister taxon of *Sericania* is according to the tree topology of the present analyses still without result; this might be a consequence of the Asian sericine fauna still being fragmentarily known, but also of the fact that, as evident also from other similar studies (chapter 3.1 and unpublished results), morphological characters of Sericini have been found to be only hardly suitable to resolve basal nodes of major species groups or genera in respect to the high number of taxa (~ 200 genera of Sericini presently described from Palaeotropical region; Ahrens unpublished).
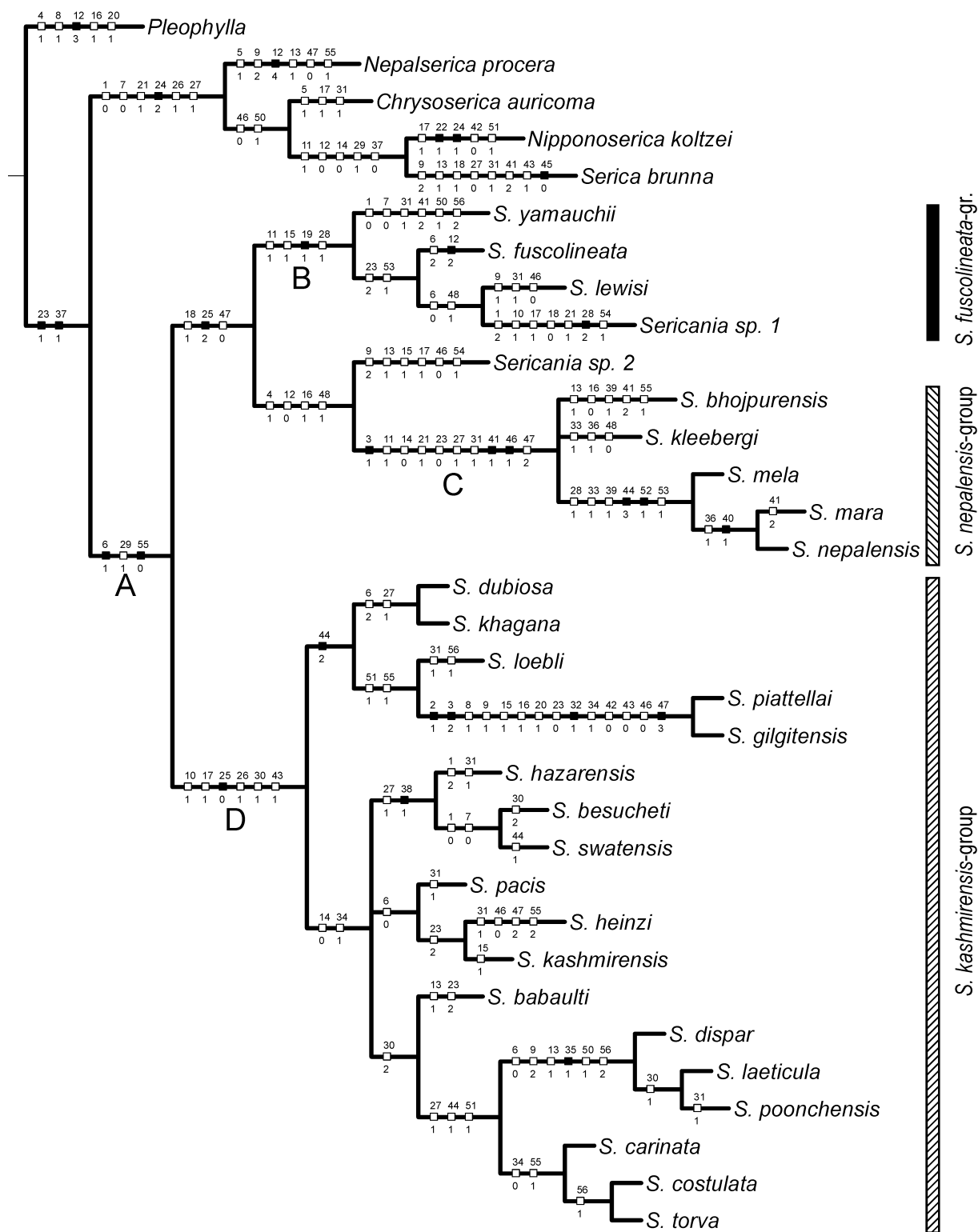
Fig. 77. Phylogeny of *Sericania*. Strict consensus (173 steps, CI: 0.54, RI: 0.78) tree of six equally parsimonious trees (172 steps CI: 0.55, RI: 0.78) resulting from successive approximation based on consistency index. Above each node branch support (bootstrap value) is indicated. *S.* = *Sericania*.
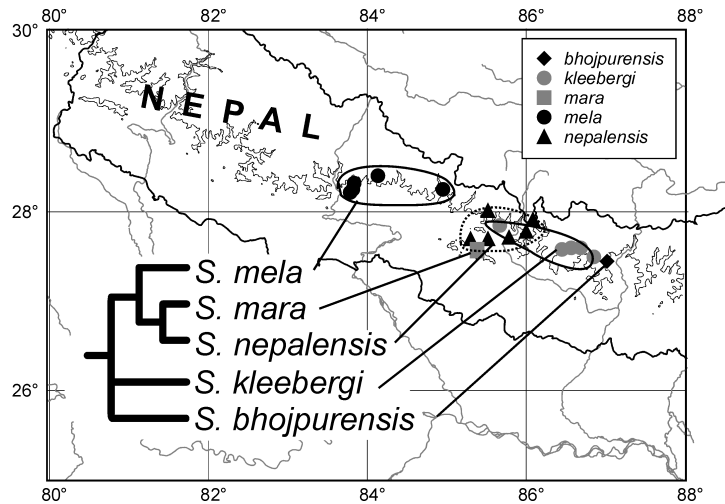
Evaluation of the clades + Evolution of Sericania

Among the three major lineages recognized from both strict consensus tree (Figs 75, 77) the *Sericania fuscolineata*-group represents the genus *Sericania* as defined 'originally' by Motschulsky (1860) and followed by subsequent authors (e.g. Medvedev 1952b; Nomura 1976). Its monophyly is best supported by following apomorphies (see node B, Fig. 78): (1) metacoxa transversely impressed (19:1); and (2) basal metatarsomere as long as the subsequent tarsomere (28:1). The species of this clade were reported from Far East Asia so far, but in the present study a still undescribed taxon (*Sericania* sp. 1) is reported also from the eastern margin of Tibetan Plateau. This species is nested in a distal position among the representatives of the group.

Fig. R6. Strict consensus (173 steps) tree of six MPTs (172 steps) resulting from successive approximation based on consistency index showing apomorphies mapped by state (discontinuous characters are mapped as homoplasy, DELTRAN optimization, unsupported nodes collapsed and using proportional branch lengths) (full squares: non-homoplasious character states; empty squares: homoplasious character states). *S.= Sericania.*

The sister taxon relationship of the *Sericania fuscolineata*-group with the second major clade of *Sericania*, the *Sericania nepalensis*-group + *Sericania* sp. 2, is based upon (1) the scutellum in comparison to elytral base narrow (18:1); and, as apparent under DELTRAN and ACCTRAN optimization (Fig. 78), (2) the metatibia at apex interiorly close to tarsal articulation sharply incised and strongly truncate (25:2). *Sericania* sp. 2 from Shaanxi (China)

shows in male genitalia several apomorphies altering in notable manner from the ground pattern of both, the *Sericania fuscolineata*-group and the *Sericania nepalensis*-group, which is reflected by the little branch support of *Sericania nepalensis*-group + *Sericania* sp. 2. Consequently, I prefer to assign *Sericania* sp. 2 not to the formally established and well supported *Sericania nepalensis*-group (node C). The areas, where *Sericania* sp. 1 and sp. 2 occur, are still poorly investigated, and additional representatives of further lineages are expected to be discovered. The representatives of the *Sericania nepalensis*-group are restricted to the Central Himalaya, where they diversified only little compared to other groups endemic in the Himalaya (Fig. 79).
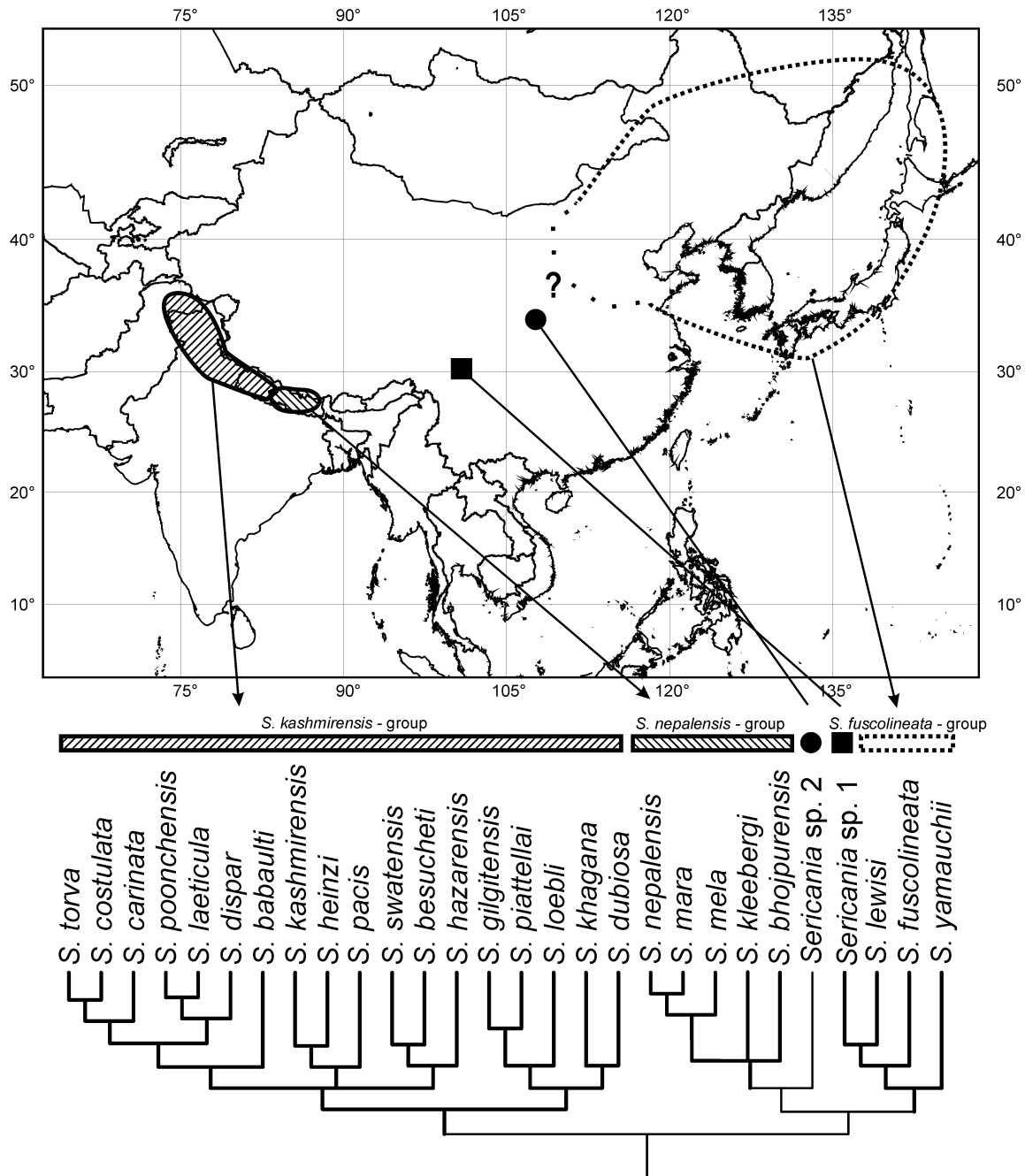

Fig. 79. Phylogeny of the *Sericania nepalensis*-group in its geographical framework, with indicated distribution of the species, and 2000 meter altitude line. *S.= Sericania.*

According to the phylogenetic hypothesis yielded from the cladistic analysis, the Himalayan *Sericania* represent not a monophyletic group, but two separate lineages. The *S. nepalensis* clade, is nested within a clade whose majority of species are East Asian (Fig. 80), which is sister taxon to the second Himalayan clade, the *Sericania kashmirensis*-group. This pattern reveals that faunal exchange must have occurred at least twice, but the direction is hardly to be determined without better knowledge of the Chinese sericine fauna.

Corroborative evidence includes the phylogenetic hypothesis of *Sericania* (Figs 75, 77) and occurrence of the three principal clades of *Sericania* (Fig. 80), indicating that the present range of the *Sericania kashmirensis*-group is a relic of a formerly wider distribution. Ranges of many of its taxa result based on the present level of exploration still fragmentary with widely isolated occurrences (Fig. 81), such as in *S. babaulti*, *S. laeticula*, or *S. hazarensis*. Closely related species (sister taxa) in several cases occur sympatrically (Fig. 81), such as *S. laeticula* and *S. poonchensis*, or are closely neighbouring, as in *S. gilgitensis* and *S. piattellai*, in *S. heinzi* and *S. kashmirensis*, in *S. costulata* and *S. torva*, or in *S. besucheti* and *S. swatensis*.

The species of the *Sericania kashmirensis*-group are with the majority of their taxa restricted to the Indus Himalaya (Troll 1972). A few taxa extend their ranges more easterly. Endemic forms are missing completely east of the Indus Himalaya. This horizontal climatic-vegetational region has an arboreal belt, which is in contrast to all other regions of the Himalaya, delimited not only in high altitude by alpine vegetational belt, but also in lower altitude (below ~ 2400 m), where desert steppe and *Artemisia* steppe are apparent (Troll 1972; Fig. 82). Most of the species of the Sericini dwell in arboreal habitats (Ahrens 2004b). As the *Sericania* species avoid the alpine belt completely, this phenomenon of altitudinal vegetational structure is supposed to be of immense importance for the capacity to survive during periods of climatic deterioration, or to disperse in adjoining areas. This might explain,
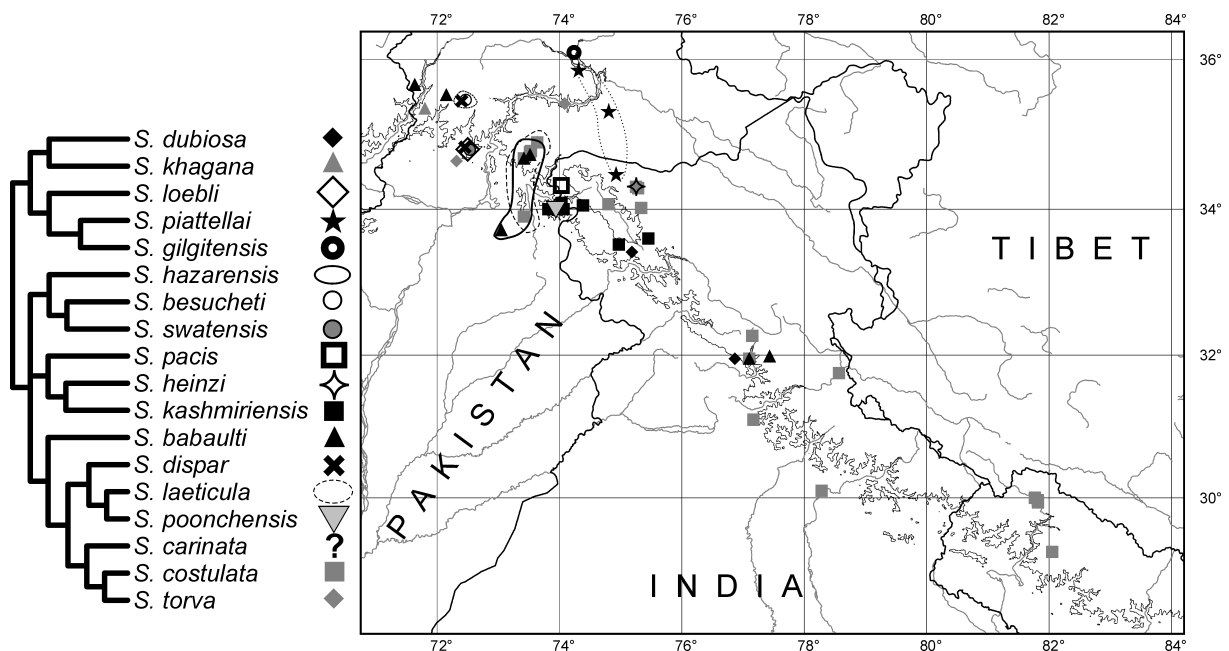
why these species adapted to aridity are so obviously restricted to the north-western Himalaya and not dispersed into drier regions of Tibetan Highland or the inner valleys of the central Himalaya, and why so closely related species occur in so nearby neighbouring areas. On the other hand, in these extreme arid habitats the competition pressure of the eastern elements of Himalayan sericine fauna is not present.

Fig. 80. Phylogeny of *Sericania* in its geographical framework. Cumulative generalized distribution of the principal lineages (with bold tree branch lines) is shown, with the respective ranges indicated as follows: *S. kashmirensis* - group: continuous line and shaded from left down to right above; *S. nepalensis* - group: continuous line and shaded from left above down to right down; *S. fuscolineata* - group: pointed line. *S.=* *Sericania*.
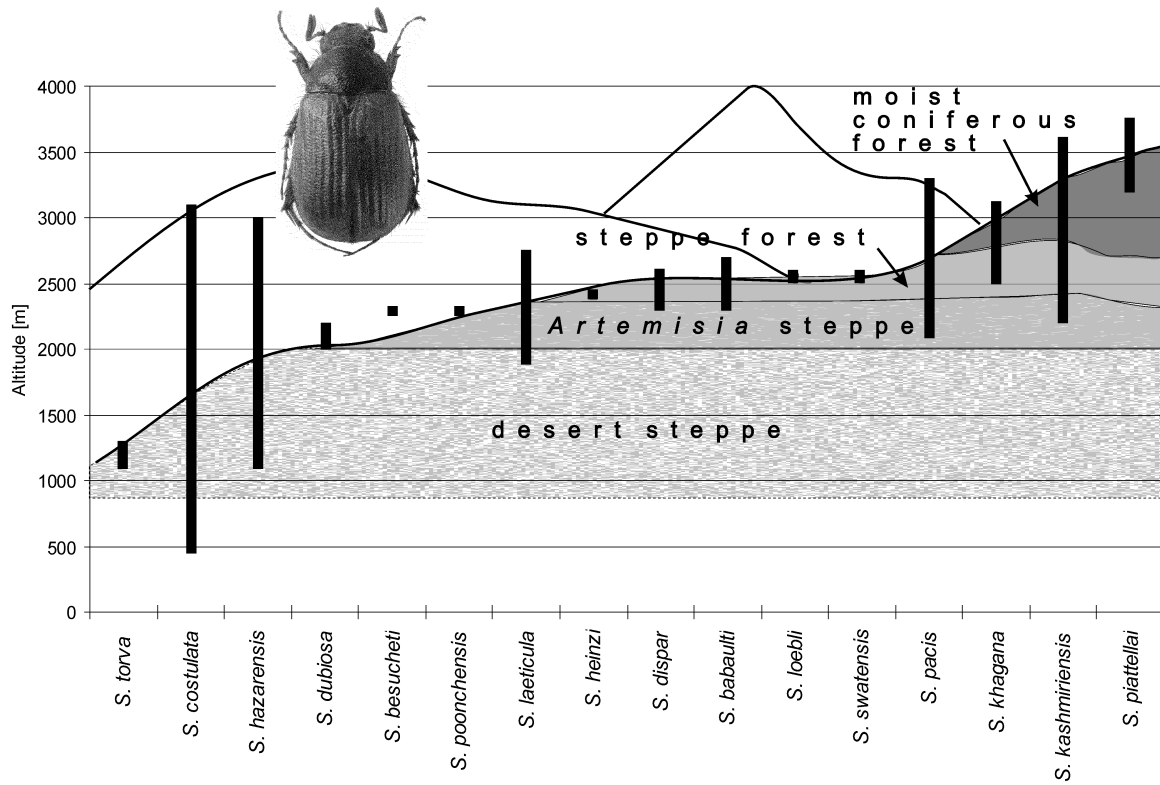
Based on the present exclusive distribution of the *Sericania kashmirensis* clade in drier parts of the North-West Himalaya I would hypothesize that the stem species of this clade was also xerophilous and less adapted to the humid conditions which are today present at southern slope of the Central and eastern Himalaya. Provided that the stem species (Fig. 78, node D) of

the *S. kashmirensis* clade was xerophilous, one conceivable hypothesis would be a range extension of the species of the *S. kashmirensis* clade along the northern margin of the rising Tibet, whose northern part is supposed to have achieved its high elevation much later (Pliocene to Quaternary) than the southern parts of the Highland (Tapponier et al. 2001), which are of relevant elevation since Eocene/ Oligocene. This range extension may predate also the onset of monsoon since about 8 Ma (Prell et al. 1992, Quade et al. 1989), as Hongfu (1994) reconstructed for Southern Tibet (+Himalaya) a humid tropical climate from Eocene to Neogene which must have been similar to the present climate at the southern slope of the Central and eastern Himalaya. The climatic divide along the Tertiary orogenic belt (southern Tibet, Himalaya) might have formed an effective barrier, if vicariance is assumed as separating event between the two basal lineages of *Sericania*. The present range of the *S. kashmirensis* clade would constitute just a relic of this formerly more expanded northern distribution.

Fig. 81. Phylogeny of the *Sericania kashmirensis*-group in its geographical framework, with indication of the distribution of the species and 2000 meter altitude line. *S. = Sericania.*

Regarding the presumably more hygrophilous stem lineage being sister taxon to the *S. kashmirensis* clade, it should be hypothesized that it has evolved close to the south-eastern margin of present Tibetan Highland, offering the stem lineage of the *S. nepalensis*-group the possibility to disperse along the southern Himalayan slope westerly, and to the *S. fuscolineata*-group north-easterly, where it performed a strong diversification on the Japanese Archipelago. Although the sister taxon of *Sericania* is unknown, a preliminary hypotheses of evolutive diversification may be discussed. The knowledge of the sister taxon of *Sericania* might bring more light on the origin of the stem species of *Sericania* and the general direction of dispersal of the several lineages.

Fig. 82. Altitudinal distribution of the taxa of the *Sericania kashmirensis* clade (*S. gilgitensis* omitted due to lacking data) in context of the climatic and vegetational zonation of the Indus Himalaya (according to Troll 1972), where the vast majority of the species of the *Sericania* occur. *S.* = *Sericania*.